EFFECTS OF NONLINEAR DISTORTION ON CDMA COMMUNICATION SYSTEMS

Seng-Woon Chen, William Panton, and Rob Gilmore

Qualcomm, Inc.
6455 Lusk Blvd., San Diego, CA 92121

Abstract — We report a rigorous approach to analyze the effects of nonlinear distortion on code division multiple access (CDMA) wireless communication systems based on time-domain analysis and band-pass nonlinearity theory. Given AM-AM and AM-PM characteristics of a nonlinear device, this technique is capable of predicting adjacent channel power rejection (ACPR), power compression, and base-band signal vector constellation at the output of the nonlinear device. To demonstrate and verify the capability of this technique, an L-band power amplifier was designed, built, tested with CDMA waveforms, and compared with the simulated results. Excellent agreement between the measured and predicted results has been achieved.

I. Introduction

`In cellular and personal communication systems (PCS), nonlinear devices, especially the power amplifier (PA), generate co-channel and adjacent channel interference due to intermodulation distortion (IMD) and side-band regrowth. In global satellite communications, stringent regulatory emission requirements in the reverse link have been proposed to prevent interference with existing navigation communication systems. Several different methods have been used to characterize nonlinear distortion of a nonlinear device and to evaluate its effects on RF system performance. Third-order intercept point (IP3) and two-tone IMD products are the most popular specifications. NPR is preferred in transponder design for commercial communication satellites to simulate multi-carrier situation. In cellular and PCS, sideband regrowth or ACPR is favorite due to its close correlation to overall system capacity. In addition, it has been found that output P_{1dB} of a power amplifier, when measured with band-limited noise like signal, such as CDMA waveform, is usually 1 ~ 2 dB below that measured with CW tone. In many cases, the power amplifier must be operated a few dB below P_{1dB} to be sufficiently linear.

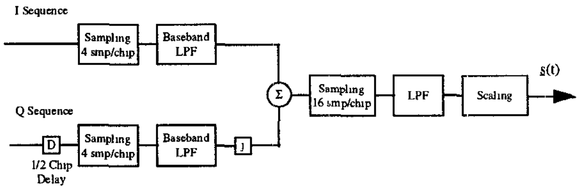

Fig.1 Simplified model of CDMA reverse traffic channel

This paper describes a time-domain approach to accurately predict side-band regrowth and power suppression caused by nonlinear devices in CDMA systems based on measurement of AM-AM and AM-PM characteristics and application of band-pass nonlinearity theory and digital signal processing techniques. Since all the calculation is done at baseband, the effect of this distortion to the overall system performance can be analyzed by examining the time-domain envelope waveforms and signal vector constellation. The material presented here will provide insight into the effects of nonlinear distortion to wireless communications and correlation among different nonlinearity specifications.

II. Principles

Fig.1 shows a simplified block diagram of the CDMA transmitter for the phone to base station link (reverse link). This transmitter is the type specified in TIA/EIA/IS-95 for cellular telephone communication and is used for PCS and global satellite communication systems as well. The digital pseudo-noise (PN) sequences that modulate the I and Q channels are modeled as two independent random number sequences with chip rate 1.2288 Mcps. The impulse response of the FIR baseband filter complies with TIA/EIA/IS-95. Before the data sequences are fed to

0-7803-3246-6/96/$5.00 © IEEE

the digital FIR baseband filters, each sequence is sampled at 4 times the chip rate as stated in IS-95. The sequences are up sampled at 16 times the chip rate with ideal interpolation to cover 8×1.2288 MHz offset at each side of the carrier frequency according to the Nyquist Theorem. An IF band-pass filter (usually in the form of a SAW filter) follows the OQPSK modulator to reduce the transmit noise floor. Since we are dealing with baseband signals, the IF band-pass filter is frequency-translated to baseband. Because a SAW filter is an FIR filter, it can be simulated digitally. The envelope waveform is scaled to the desired power level prior to being applied to the nonlinear device under analysis. In the generation of the simulated CDMA waveform, the baseband filtering is implemented in the time domain, i.e. convolution of the sampled random sequence with the impulse response of the baseband filter. The baseband filtered sequences are then Fourier transformed using the FFT algorithm and multiplied with the frequency response of the SAW filter. Finally, the CDMA baseband envelope signal is obtained by inverse FFT.

It has been shown [1] that a narrow band RF band-pass signal and system can be represented by its baseband complex envelope and response, respectively. Therefore, the analysis of a band-pass system can be replaced with an equivalent low-pass analysis and retains the essence of filtering process. According to band-pass nonlinearity theory, the output complex envelope $\underline{y}(t)$ is related to the input complex envelope $\underline{s}(t)$ as follows [2]-[4]

$$\underline{y}(t) = a(t)\left[G(a(t))\right] \cdot e^{j\{\phi(t)+P[a(t)]\}} \qquad (1)$$

where G(a) is known as AM-AM distortion or simply gain versus input power and P(a) is referred to as AM-PM distortion. The input complex envelope $\underline{s}(t)$ can be expressed in the form of

$$\underline{s}(t) = a(t)\ e^{j\phi(t)} \qquad (2)$$

where a(t) and ϕ(t) represent amplitude and phase of the input waveform are both real-valued and low-pass functions.

From equation (1), the output complex envelope and hence the real-valued signal of a nonlinear device can be derived from the input waveform and measurement of AM-AM and AM-PM distortion of the nonlinearity. AM-AM and AM-PM of an amplifier can be measured directly on a network analyzer using a CW power sweep. For narrow band RF communication systems, measurement at a single frequency is usually sufficient.

To predict the effects of nonlinearity on a CDMA system, a baseband complex envelope for the CDMA signal is first generated and scaled. In generation of $\underline{s}(t)$, 256 bits of digital data are generated for each I and Q channel independently using two random number generators. Each bit of 0 is represented by −1V, and 1 is represented by 1V. Since 256 chips are generated for each channel, the complex envelope $\underline{s}(t)$ is represented by a discrete complex sequence $\underline{s}[n]$ of N=16×256=4096 samples. Using the measured AM-AM and AM-PM distortion and generated complex envelope samples $\underline{s}[n]$, the output complex envelope sequence $\underline{y}[n]$ of the PA can be derived from equation (1). Adjacent channel power rejection (ACPR) of the power amplifier output can be obtained with power spectrum analysis [5]

$$S_{\underline{y}}[k] = \frac{\left|\underline{Y}[k]\right|^2}{N^2} \qquad k = 0, 1, \ldots N-1 \qquad (3)$$

where $S_y[k]$ is the power spectral density (PSD) of $\underline{y}[n]$ over the resolution bandwidth Rb = 16×1.2288/4096 = 4.8 kHz, and $\underline{Y}[k]$ is FFT of $\underline{y}[n]$. The output power P_{out} of power amplifier can be calculated as follows

$$P_{out} = 10\log\left[\frac{1}{N}\sum_{n=0}^{N-1}\left|\underline{y}[n]\right|^2\right] = 10\log\left[\frac{1}{N}\sum_{k=0}^{N-1}\left|\underline{Y}[k]\right|^2\right] \qquad (4)$$

III. Simulation and Measurement Results

To demonstrate the capability of the IMD simulation technique, we designed, built, and tested an L-band two-stage hybrid power amplifier using Fujitsu's FLL011ME as the first stage device and FLL351ME for the second stage. Fig.2 shows the AM-AM and AM-PM of the PA measured with the built-in CW power sweep function of the HP8753D network analyzer. For accurate simulation on the compressed region, the CW power sweep has to extend to at least 5 dB beyond P_{1dB} to account for the peaks in the baseband envelope signal due to baseband pulse-shaping filtering. Fig.3 shows the predicted and measured output power spectrum density over 16 MHz bandwidth at input powers of 1 and 5 dBm. The measurement is made using the HP8920A RF Communications Test Set with the HP83203A CDMA

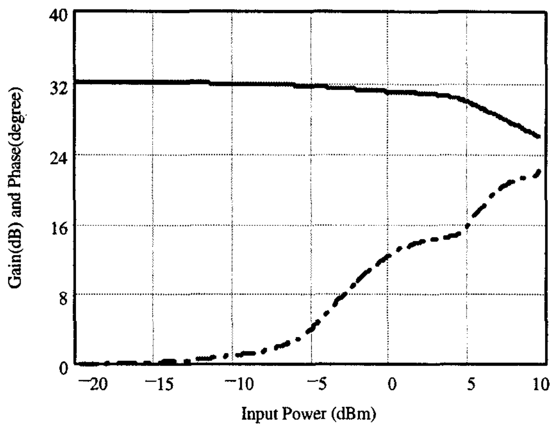

Fig.2 Measured AM-AM (solid line) and AM-PM (dash-dot line) of an L-band power amplifier.

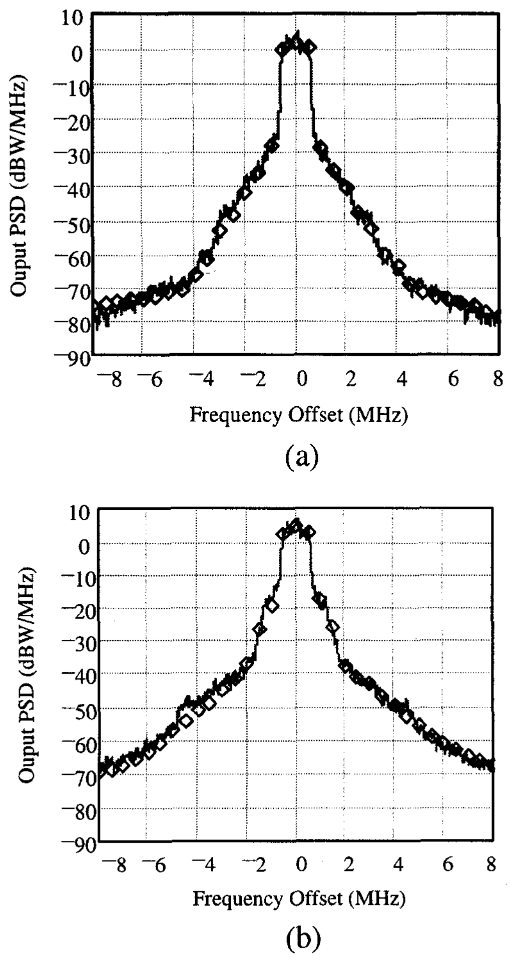

Fig.3 Power spectrum density curves at output of the PA (a)Pin=1dBm, Pout = 31.9dBm, (b)Pin = 5dBm, Pout = 34.3dBm. Carrier frequency = 1610.875 MHz. (Solid lines: Simulation, Diamonds: Measurement)

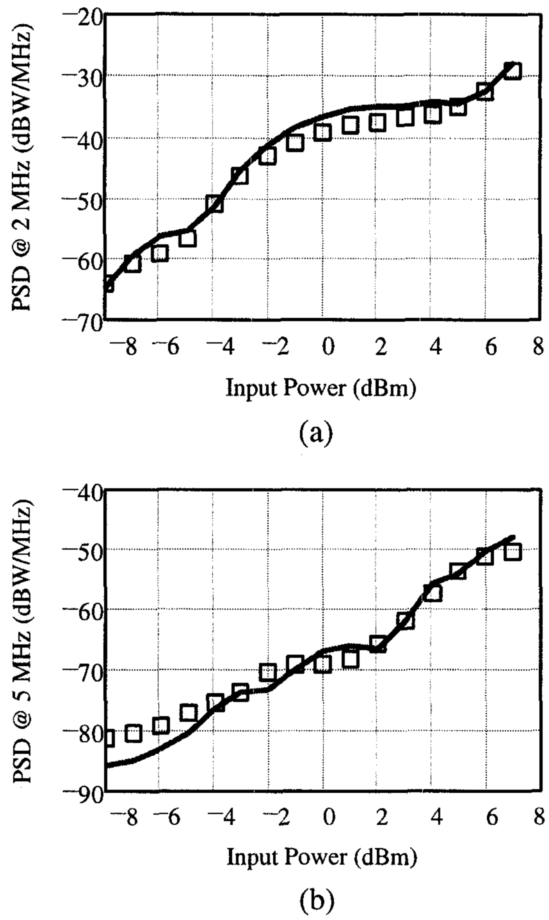

Fig.4 Power spectrum density at (a) 2 MHz offset, and (b) 5 MHz offset as a function of input power. Carrier frequency=1610.875 Mhz. (Solid lines: Simulation, Squares or Boxes: Measurement)

Cellular Adapter to generate the reverse link, CDMA Waveform. Therefore any error that might be introduced by simulating the digital PN sequences with random number generators will be apparent in the results. Adjacent channel power rejection and RF emission at any frequency offset within the simulation bandwidth can be easily seen from the PSD plots. Fig.4(a) and (b) present the PSD at 2 and 5 MHz offset from the carrier frequency, respectively. Excellent agreement between the predicted and measured results has been achieved as show in the figures.

Fig.5 shows comparison of simulated with measured P_{out}-P_{in} transfer curves with CW carrier and CDMA signal. At low input power drive, the PA is operating on the linear region so the gain is amplitude-invariant and the output power is the same as measured from CWcarrier. At higher power drive, the gain is more compressed at the time instant when the envelope waveform exhibits peaks due to baseband filtering. From equation (1), it is apparent that power

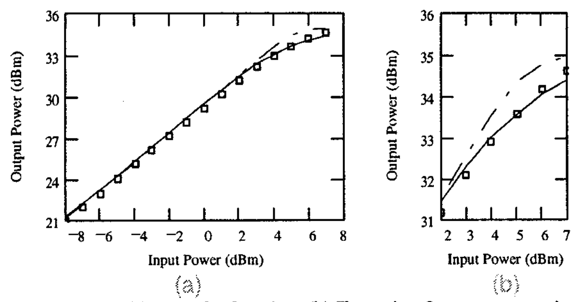

Fig.5 (a) Pout vs Pin transfer function. (b) Zoom-in of near compression. Solid line: CDMA predicted, Box: CDMA measured, Dash-dot: CW.

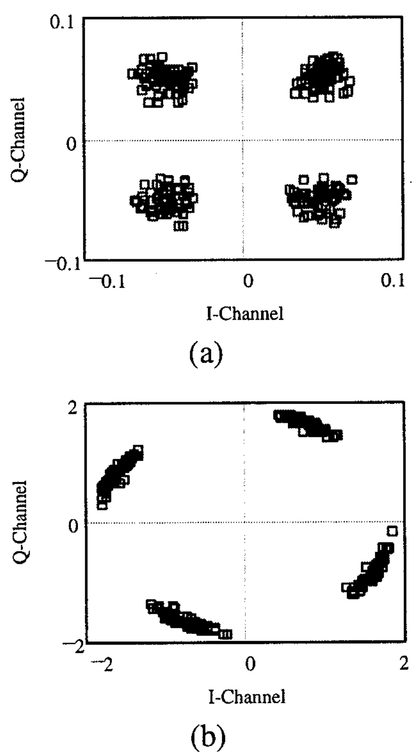

Fig.7 (a) Input and (b) Output signal vector constellation, PA input power = 7 dBm.

suppression of CDMA waveform depends on AM-AM distortion and peak-to-average ratio of the envelope signal.

The effects of nonlinear distortion generated by a power amplifier can be visualized with the time-domain waveforms. Distortion of the signal can be presented in a signal constellation diagram. Fig.6 shows the QPSK signal constellation at the input and output of the PA when the input drive is equal to 7 dBm. No timing error is assumed in this simulation. In Fig.6(b), the signal is compressed inwards due to amplitude distortion and rotated and spread due to phase distortion. If large number of chips is simulated, at some time instants, the signal points may move from one quadrant to another and cause bit errors.

IV. Conclusion

We have demonstrated a time domain approach to analyze nonlinear distortion based on band-pass nonlinearity theory and digital signal processing techniques. The analysis technique has been implemented with Math Soft's Mathcad. To demonstrate the capability of the IMD simulation technique, we designed and built an L-band two-stage hybrid power amplifier. Measurement on power spectrum density and power suppression has been performed with CDMA waveforms to verify the analysis and shows excellent agreement. The effects of PA's nonlinearity on the overall RF communication system performance were visualized by examining signal vector constellation.

The analysis technique described here applies not only to power amplifiers but also to any other nonlinear components such as mixers and switches. This approach can also be used to predict IMD products and NPR without any notch filter. The approach is also well suited to analyze nonlinear distortion in base station and satellite transponder power amplifiers, where the input signals are usually multiple-channels with a different power level for each channel.

Reference

[1] S. Haykin, *Communication Systems*, 2nd ed., John Wiley & Sons Inc., 1983.

[2] N. M. Blackman, "*Band-Pass Nonlinearities*," IEEE Trans. on Information Theory, Vol. IT-10, Apr. 1964, pp. 162-164.

[3] N. M. Blackman, " *Detectors, Bandpass Nonlinearities, and Their Optimization: Inversion of the Chebyshev Transform*," IEEE Trans. on Information Theory, Vol. IT-17, Jul. 1971, pp. 398-404.

[4] O. Shimbo, " *Effects of Intermodulation, AM-PM Conversion, and Additive Noise in Multicarrier TWT Systems*," Proc. of IEEE, Vol. 59, No. 2, Feb. 1971, pp. 230-238.

[5] A. V. Oppenheim and R. W. Shafer, *Discrete-Time Signal Processing*, Prentice Hall, New Jersey, 1989.